



Optimisation of driver actions in RWD race car including tyre thermodynamics

Michal Maniowski

To cite this article: Michal Maniowski (2016): Optimisation of driver actions in RWD race car including tyre thermodynamics, Vehicle System Dynamics, DOI: [10.1080/00423114.2016.1158411](https://doi.org/10.1080/00423114.2016.1158411)

To link to this article: <http://dx.doi.org/10.1080/00423114.2016.1158411>



Published online: 21 Mar 2016.



Submit your article to this journal [↗](#)



Article views: 37



View related articles [↗](#)



View Crossmark data [↗](#)

Optimisation of driver actions in RWD race car including tyre thermodynamics

Michal Maniowski

Institute of Automobiles and Internal Combustion Engines, Cracow University of Technology, Cracow, Poland

ABSTRACT

The paper presents an innovative method for a lap time minimisation by using genetic algorithms for a multi objective optimisation of a race driver–vehicle model. The decision variables consist of 16 parameters responsible for actions of a professional driver (e.g. time traces for brake, accelerator and steering wheel) on a race track part with RH corner. Purpose-built, high fidelity, multibody vehicle model (called ‘miMa’) is described by 30 generalised coordinates and 440 parameters, crucial in motorsport. Focus is put on modelling of the tyre tread thermodynamics and its influence on race vehicle dynamics. Numerical example considers a Rear Wheel Drive BMW E36 prepared for track day events. In order to improve the section lap time (by 5%) and corner exit velocity (by 4%) a few different driving strategies are found depending on thermal conditions of semi-lick tyres. The process of the race driver adaptation to initially cold or hot tyres is explained.

ARTICLE HISTORY

Received 10 August 2015
Revised 21 February 2016
Accepted 22 February 2016

KEYWORDS

Optimisation; thermal behaviour; driver–vehicle systems; driving simulator; tyre dynamics

1. Introduction

The temperature of performance tyre tread, in dry track conditions, may be responsible for [1]:

- a lower grip of not warmed (tyre slips) or overheated (tyre ‘flows’ and wears rapidly) tyres;
- a rise time in response, often misinterpreted as an effect of a car body dynamics;
- an oversteering of front wheel drive (FWD) car at a corner entry, after a long straight that cools rear tyres more;
- an understeering of rear wheel drive (RWD) car at a corner entry, after a long straight that cools front tyres more.
- a premature overheating of the front tyres in FWD car (with 60/40 mass distribution);
- more even distribution of tyres temperature between the axles in RWD car (50/50);
- tyre flat spot on locked wheel (local overheating degrades average grip and tread profile).

The temperature of tyre tread varies during a race vehicle motion. Sample time traces of tyre tread temperature, measured by a pyrometer on instrumented BMW E36 during a hot day (35°C) track session (on centre line of front RH tyre with semi-slick Michelin SA20), are presented in Figure 1.

The tread temperature rises slightly when braking (at $t = 20$ s, Figure 1) and considerably when cornering on LH turns (at $t = 24$ s and $t = 36$ s, Figure 1) with peak temperature delayed with respect to a corner apex and maximal temperature gradient up to 20°C/s. Tyre tread cools down even faster on straight sections when the vehicle accelerates (at $t = 27$ s, Figure 1), as well as on RH turns (unloaded wheel).

Several factors may affect the tyre temperature, namely [2]: wheel normal load and slip, average speed, airflow around the tyre, road temperature, air temperature, heat transmitted from brakes or engine, tyre pressure, tyre tread thickness, tread pattern, rubber compounds and tyre construction.

A typical distribution of a tread flash temperature (T_t) in the tyre circumferential direction is presented in Figure 2 – left.[3] The tread tip heats up in a sliding zone of the contact patch proportionally to sliding velocity profile. It reaches the highest temperature at the end of the contact patch. Subsequently, a heat exchange process starts through a convection (cooling for $T_t > T_a$) from a free tread surface at the tyre circumference to an ambient air. Another heat transfer is caused by a conduction in radial direction between the tyre tread and the carcass with a gas volume. This heat-flow path is described by rather a high level of isolation due to material properties of the rubber. The heat exchange process can be also continued in a leading edge of the contact patch in an adherent zone due to a conduction between the tread tips and the road surface (with temperature T_r). The tread temperature may have an unequal distribution in lateral direction of the contact patch, which is treated as a major clue for adjusting settings of the wheel camber angle and the tyre internal pressure.

One of the most important tyre characteristics in motorsport applications is the relation between the peak friction value (grip) and the tyre tread temperature (T_t), which

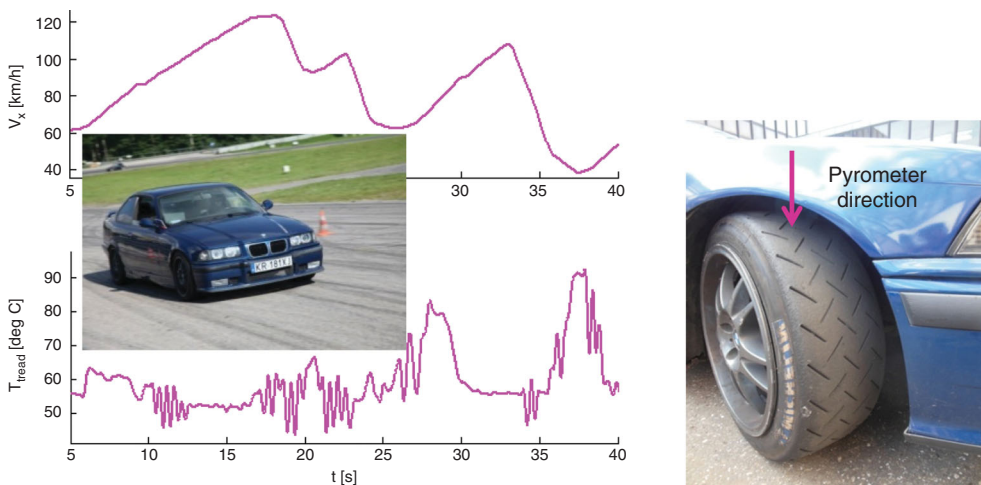


Figure 1. Measured temperature of FR tyre tread and velocity traces of BMW E36 during a race session.

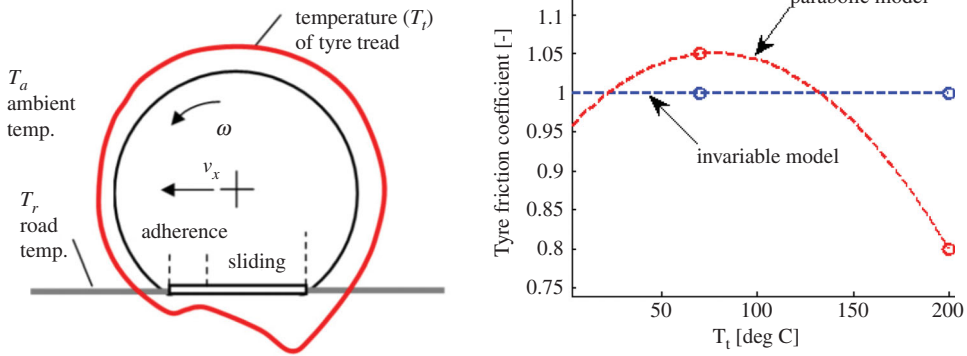


Figure 2. Tyre model with tread temperature variation (left) and its influence on tyre grip (right).

usually is described by a parabolic function, like in Figure 2– right. The optimum grip temperature depends on a glass transition temperature of a rubber mixture, among the others. [4] Regular road tyres have a lower and more flat peak, placed at lower temperatures according to its operating ranges. The competition (slick, semi-slick) tyres are described by a more profound peak placed at a higher temperature, depending on application (e.g. racing, qualifying, rally and drifting).

Developments in the field of software for analysis of extreme handling manoeuvres, training simulators and lap time optimisation require a detailed description of the tyre thermodynamics. Selected tyre models with thermo-effects are compared in Table 1 and described beneath.

In 2003 Mizuno [5] developed for Toyota a tyre side force model based on ‘Magic Formula’ with the influence of tyre surface temperature. In his work, thermodynamics of a substitute mass of the tyre tread, which is heated by a lateral slip and cooled by an environment, is considered. The computed tread temperature is incorporated in magic formula (MF) coefficients describing the tyre lateral grip and cornering stiffness. This approach has the simplest structure and hence low computational and estimation time.

Chaligné [6] proposed an empirical temperature model. The tyre temperature is estimated in real time by a quadratic function based on input parameters (slip and camber angles, vehicle speed, pressure and normal load). Unknown coefficients are determined experimentally by means of indoor experiments. The determined tread temperature is incorporated in the MF model coefficients describing tyre lateral grip and cornering stiffness. The proposed formula is computationally effective, but poses questions about estimation time and extrapolation errors.

The following model belongs to a group with hybrid structure, which combines physical finite element analysis (FEA) principles with empirical sub-models of certain tyre components. In MuRiTyre [7] the contact patch is discretised by longitudinal ribs (at least 3) generating individual normal and tangential stress profiles and tread temperatures. The contact patch is linked with a tyre carcass modelled by quasi FE. MuRiTyre is dedicated to motorsport, including simulators, but described sparingly.

Another example of a hybrid model is TaMeTirE (Thermal and Mechanical Tire Emulator), [3] utilised by Michelin to predict tyre loads during vehicle manoeuvres,

Table 1. Comparison of tyre models with thermo-effects for handling analysis or lap time simulators.

Features	'Toyota' [5]	Chaligné [6]	MuRi [7]	TaMe [3]	FTire [8]	TRT [9]
General structure	Single mass	Empirical temp. model	Hybrid	Hybrid	MBS	FEA
Tyre tread temp. in contact patch	Single mean temp.	Single temp.	Single temp. for each rib	Distributed 3D	Distributed 2D	Distributed 3D
Tyre tread temp. out of patch	No	No	(?)	Single temp.	Single temp.	(?)
Tyre carcass temp.	No	No	(?)	No	Single temp.	(?)
Internal air volume temp.	No	No	(?)	Pres = f (temp.)		(?)
Temperature influences on	Grip, cornering stiffness	Grip, cornering stiffness	Grip, rubber shear module	Grip, rubber shear module, tread wear	Grip, tread wear	Grip
Exchange of heat with	Environment	Air in wheel house	(?)	Air, road	Air, road	Air, road
Heating sources	Lateral slip	Slip, camber, velocity, pressure, normal load	(?)	Slip, internal heating	Slip, internal heating	Slip, internal heating
Computation cost	Low	Low	Medium (real time)	Medium (real time)	Higher	High
Estimation cost	Low 3 params	Medium (?) params	Medium (?) params	High (?) params	Medium 6 params	Medium

especially at the limit of friction (e.g. safety manoeuvres, lap time and braking). Due to a physically based structure composed of three parts (mechanical, rubber and thermal), the model parameters are more directly related to the actual tyre construction, than to fitting curves to test machine results. Temperatures of tyre tread can be computed as a 3D distribution along the tread surface and the tread thickness.

In commercial software FTire [8] (Flexible Structure Tire Model) a 3D flexible tyre structure is modelled as a multi body system (MBS), composed of thousands rigid elements. This approach can be still faster by orders of magnitude than explicit FE models, but real-time application is a challenge. The thermal model in FTire can compute: temperature distribution (in 2D) on the tyre tread in contact patch, single temperature for the free tyre tread and single temperature for the tyre structure (side-wall, belt, and air volume).

The last example is related to Thermo Racing Tyre (TRT),[9] which is based on the FE carcass model. The model can calculate the temperature distribution in different tyre layers (surface, bulk and inner liner) and estimates local grip values. This model may be useful during the design phase of the tyres, as well as in choosing the tyres according to the various circuits characteristics. It is stated that the model has a computational capability for real-time applications.

This paper presents an innovative method of a performance driver optimisation to improve the lap time with focus on tyres thermal effects. Typically, these features are adapted based on many track tests with trial and error methods. In order to fasten this process, the 'miMa' simulation model of vehicle–driver–road is subjected to optimisation

involving genetic algorithms. In comparison with the other known procedures addressing the problem of lap time minimisation, [10,11] ‘miMa’ is characterised by:

- (a) combined optimisation of driver actions for closed-loop manoeuvres, vehicle chassis parameters and motion trajectory;
- (b) no need of an oversimplified race driver model, i.e. actions of a real driver are acquired from track measurements and afterwards introduced as additional decision variables in the optimisation, which results in more realistic emulation of the driver adaptation process;
- (c) multibody, high fidelity model of vehicle with discrete parameters specialised in motorsport;
- (d) optimal balance between model accuracy and computation time (real-time factor = 0.3);
- (e) implementation of genetic algorithms, enabling a global search of a highly nonlinear task;
- (f) decision variables with mixed continuous–discrete domain.

The goals of this paper are focused on:

- modelling approach of basic thermal effects in tyres for vehicle dynamics studies;
- enhancing a race driver capability to fully exploit tyres with a variable tread temperature by means of the optimisation of the driver–vehicle–road model.

2. ‘miMa’ model of the driver–vehicle–road system

2.1. Definition of the ‘miMa’ model

The model of the driver–vehicle–road system (Figure 3) adapted for optimisation problems is formulated by the author in Matlab environment. ‘miMa’ is characterised by deep specialisation in motorsport applications, e.g. rally, [12] race, [13] drifting [14] and off-road. [15] The vehicle model relates its design parameters (\mathbf{p}) and driver actions (δ) with the vehicle dynamic characteristics, which can be derived based on its motion states (\mathbf{q} , $\dot{\mathbf{q}}$, $\ddot{\mathbf{q}}$). A multibody dynamic model with discrete parameters is described by system of nonlinear ordinary differential equations (ODE). Special formulation of closed-form solutions of the wheel suspensions makes it possible to avoid time consuming differential algebraic equations (DAE).

The virtual racing driver (Figure 3) has to guide a vehicle through a desired path, stabilise it and seek a maximum performance from a vehicle on a specific road surface. The driver actions are described by

$$\delta = [\delta_h \delta_b \delta_a \delta_c \delta_g \delta_e]^T, \quad (1)$$

where δ_h – steering wheel angle (deg); δ_b – normalised position of brake pedal ($\delta_b \in <0,1>$); δ_a – norm. position of accelerator pedal ($\delta_a \in <0,1>$); δ_c – norm. position of clutch ($\delta_c \in <0,1>$); δ_g – gear shift position ($\delta_g \in \{-1, 0, 1, 2, \dots\}$); δ_e – normalised position of e-brake ($\delta_e \in <0,1>$).

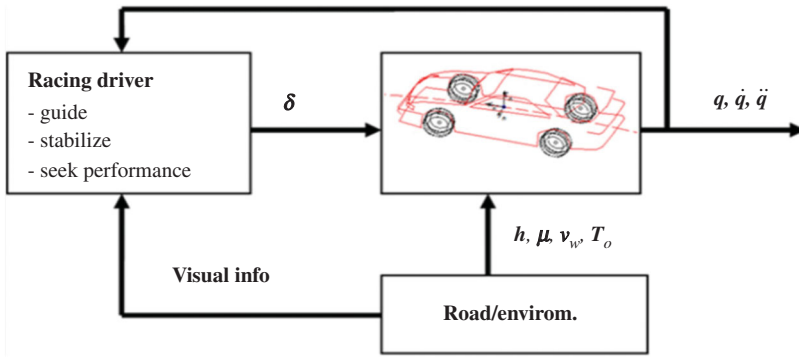


Figure 3. ‘miMa’ model of the driver–vehicle–road system used for optimisation tasks in motorsport.

The driver actions (1) are based on observations (Figure 3) of selected vehicle motion states (ζ) and visual perception. The road–environment model includes descriptions of road profiles (h), friction potential (μ), wind velocity (v_w) and ambient air temperature (T_a) and road surface temperature (T_r).

2.2. ‘miMa’ model of RWD racing car (BMW E36)

The numerical example is based on the study of a BMW E36 Coupe (with mass: 1400 kg; mass distribution: 50/50; power: 200HP, powertrain: RWD with limited slip differential; tyres: 205/45/17 semi-slick Michelin SA20, 2.2bar; ABS and Traction Control: off) prepared for track racing (see Figure 1). The nonlinear multibody vehicle model is presented in Figure 4. Main components of the ‘miMa’ model are defined in Table 2. The model, described by 30 generalised coordinates (q) and 440 discrete parameters, is suitable for dynamic analyses in a frequency range up to 20 Hz.

The most crucial chassis parameters in motorsport are related to tyres and wheel suspensions.

Wheel suspension mechanisms are thoroughly described by kinetic-static models.[16] Views of kinematic models of the front and rear BMW E36 independent suspensions are presented in Figure 4. The front wheel suspension is composed of a McPherson strut with lower L-type wishbone and the rack-and-pinion steering system positioned in front of the car. The rear wheel suspension, referred to as spherical, is composed of two lateral arms and one longitudinal fixed with the wheel knuckle.

Table 2. Description of ‘miMa’ model components for dynamic analysis of BMW E36.

Model parts	Generalized coordinates (q)	Description
Car body	6 ($x, y, z, \varphi, \theta, \psi$)	Position and orientation of rigid body
Wheels	4 ($\varphi_1, \varphi_2, \varphi_3, \varphi_4$)	Rotation about wheel bearings
Suspensions	4 (z_1, \dots, z_4)	Bounce motion
Tyres	4 + 4 + 4 ($F_{x1} \dots F_{x4}, F_{y1} \dots F_{y4}, T_{t1} \dots T_{t4}$)	First-order dynamics of tyre horizontal forces and tyre tread temperatures
Steering sys.	1 (φ_k)	Compliance of steering shaft
Powertrain	1 + 1 + 1 ($M_s, \varphi_m, \varphi_w$)	Engine torque + differential + compliance of shafts
SUM	30	

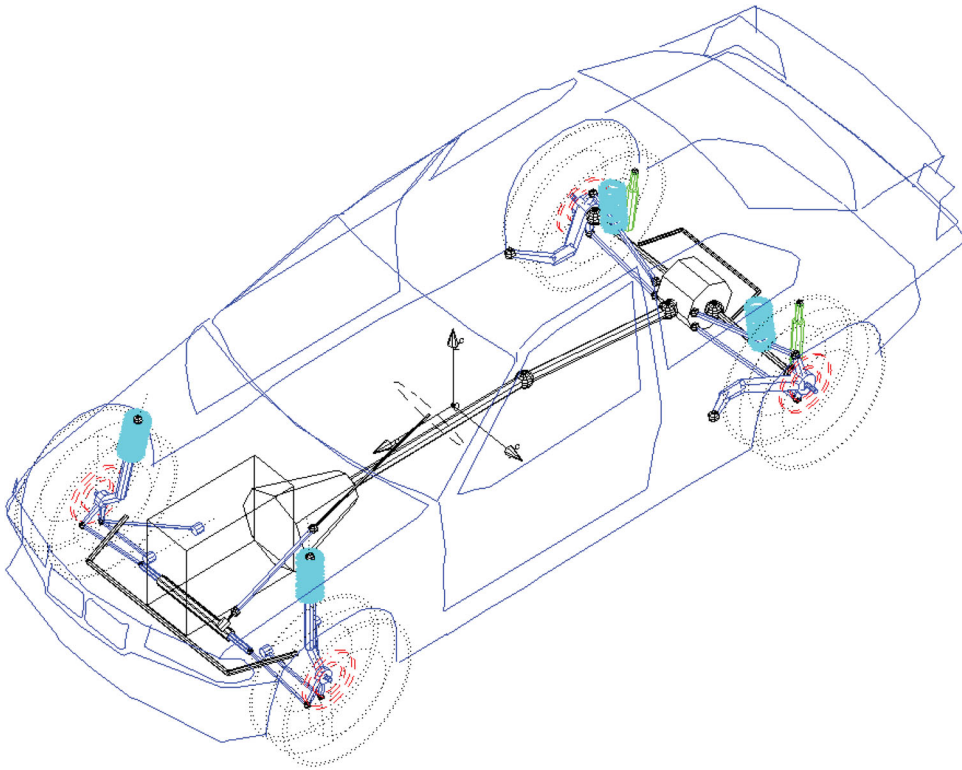


Figure 4. 'miMa' model of BMW E36 Coupe with strut and spherical wheel suspensions.

The forward kinematics problem (given: mechanism dimensions and active joint coordinates; sought: wheel pose) for the both types of wheel suspensions (strut type and spherical) is solved in a closed form. The mechanism Jacobian matrix (derived as differential of the mechanism constraints equations) is utilised to solve the statics problem (given: tyre load; sought: suspension reactions). Such a kinetic-static approach, solved in closed form, is significantly more time effective, than a general multibody approach, resulting in DAE. The effects of the suspension joints compliance are not considered here, due to an application of stiffer joints with polyurethane inserts.

Major dimensions of the actual suspension mechanisms are measured directly. Those difficult to measure are identified by comparison of kinematic characteristics (for bounce and steering motion) obtained from measurements and simulations.[17]

Characteristics of the wheels suspension springs (coil springs, bumpers and anti-roll bars) and dampers (Figure 4) are determined on the basis of test bench measurements and described as passive elements with nonlinear characteristics.

2.3. Tyre model with variable tread temperature

Tyre horizontal forces and self-aligning torques are generated by semi-empirical 'Magic Formula' [18] with complex slip conditions, relaxation lengths in longitudinal and lateral

directions. Improved characteristics of tyre friction as functions of the wheel camber and the wheel load are introduced.

The basic MF tyre model is extended to cope with thermal effects by using the method mentioned in the introduction as ‘Toyota’ model [5] (see Table 1). Assumptions for this model are as follows:

- tyre rotates ($\omega \neq 0$);
- tyre tread in contact patch is described by thermodynamics of a single lumped mass with single (mean) temperature;
- slip (longitudinal and lateral) in tyre contact patch generates main heat;
- tyre tread mass exchanges heat with environment (air and road);
- heat flow to environment is proportional to vehicle velocity (v_x) and
- tyre tread temperature influences only a peak value of friction coefficient, which is modelled by a parabolic function (Figure 2– right) with peak 1.05 at $T_t = 80^\circ\text{C}$.

Thereafter, the tread temp. (T_t) may be described by a first-order differential equations for all tyres:

$$H \frac{dT_{t,i}}{dt} = (F_{y,i} v_x \tan(\alpha_i) + F_{x,i} v_x s_{x,i}) - k_1(1 + k_2 v_x)(T_{t,i} - T_A)[W], \quad i = 1 \dots 4. \quad (2)$$

where: H – thermal capacitance (J/K); F_y – lateral force (N); v_x – vehicle velocity (m/s); α – slip angle (rad), F_x – longitudinal force (N); s_x – long. slip, k_1 – substitute coefficient of convection to environment (W/K), k_2 – substitute coefficient of velocity influence on convection (s/m), T_A – ambient temperature (mean temperature of air and road) ($^\circ\text{C}$).

There are only three coefficients (H, k_1, k_2) in Equation (2), which need to be estimated on the basis of any road tests resulting in reasonable variations of tyres temperature (from pyrometers) and vehicle velocity. The coefficient H (thermal capacitance) can be treated as a time lag of the first-order system (2). The coefficients k_1 and k_2 are responsible for a heat exchange between tyre and environment.

2.4. Verification of the ‘miMa’ model on RH corner

Most of the model chassis parameters are estimated on the basis of indoor experiments in the Institute Labs. The results of the road tests (e.g. straight acceleration, braking and quasi-static cornering) are utilised to estimate parameters for the MF tyre model with the introduced thermodynamic extension.

Verification results related to the selected track section (Figure 5), described by smooth, even and isotropic road surface with medium grip and ambient temperature $T_a = 35^\circ\text{C}$, are presented in Figure 6. The results of track test measurements involving an expert driver are compared with the simulation (without temperature effects). Two experimental trials are enclosed in the diagrams proving a high consistency of the measurement system and the driver. The driver actions ($\delta_a, \delta_b, \delta_h$ – from wire base sensors), five states of the vehicle gross motion (v_x, β_{rear} – from optical velocity sensors, and $\psi_{\text{prim}}, a_x, a_y$ – from inertial platform), temperature (T_t – from pyrometer sensor) of the FR tyre tread and deflection (s_z – from wire base sensor) of the FR wheel suspension, are presented in time domain in Figure 6.

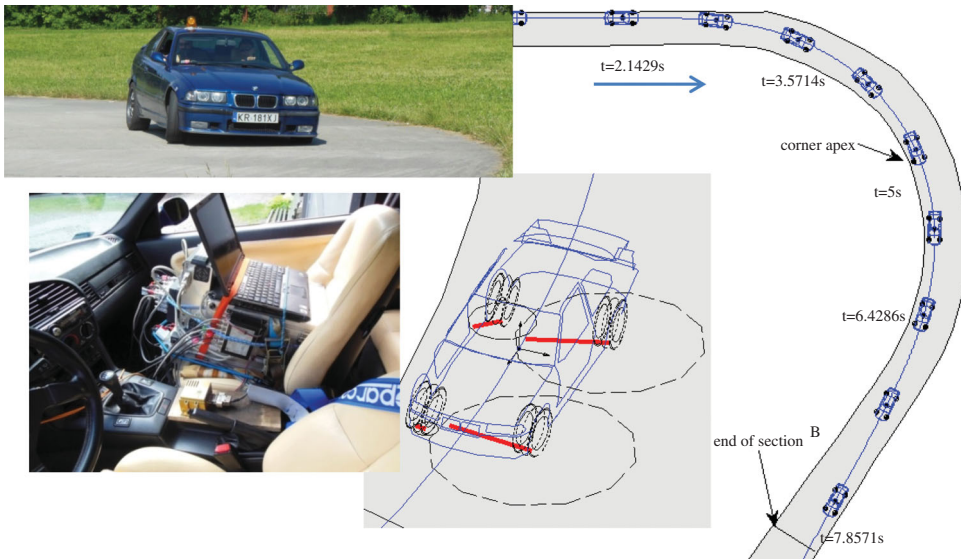


Figure 5. 'miMa' model of BMW E36 on selected section of race track with RH corner.

The manoeuvre under examination begins on a straight section A with ca 105 km/h initial velocity (v_x in Figure 6(e)). Consecutively, the car is slowed down to ca 60 km/h by applying brakes for 3 s (δ_b in Figure 6(a)) and down shifting (third to second using the heel and toe method), achieving deceleration (a_x in Figure 6(f)) on a level of -7 m/s^2 . This braking process causes a compression (s_z in Figure 6(h)) of the FR wheel suspension by only 15 mm due to stiff springs and anti-dive geometry of the front axle. Although, the wheel is under loading and braking the temperature (T_t in Figure 6(d)) of FR tyre tread increases only by a few degrees from initially 46°C to 50°C . It may be explained by a relatively low longitudinal slip achieved during this under-limit braking.

In the following phase, the driver overlaps braking with the steering action (δ_h in Figure 6(b)), which is also known as a trail braking, in order to effectively initiate a turn-in into the RH corner. The lateral acceleration (a_y in Figure 6(f)) grows to a maximum available value (-8 m/s^2) and the yaw velocity (ψ_{prim} in Figure 6(c)) reaches -32 deg/s , whilst the vehicle approaches the corner apex (Figure 5). In this phase, the FR wheel is maximally unloaded, which corresponds to rebound deflection (s_z in Figure 6(h)) of the wheel suspension by 22 mm. The temperature (T_t Figure 6(d)) of FR tyre tread this time also increases insignificantly (from 49°C to 54°C) as a consequence of a combination of increased lateral slip and decreased normal load of the tyre.

Next, the driver gradually applies the acceleration pedal (δ_a in Figure 6(a)) and reduces the turn angle, heading the vehicle to the corner exit with a small drift angle ($\beta_{\text{rear}} = -8 \text{ deg}$ in Figure 6(g)). The FR tyre tread (T_t in Figure 6(d)) cool downs very fast in this phase of the wheel free rolling. The described strategy is typical for performance driving of a RWD vehicle. The manoeuvre finishes after 7.8 s when crossing the section line B (Figure 5) with velocity $v_x = 78 \text{ km/h}$ (in Figure 6(e)).

In order to simulate the considered manoeuvre (c0) the driver actions (Figure 6(a) and 6(b): δ_h – steering wheel, δ_b – brake pedal, δ_a – accelerator) are approximated by

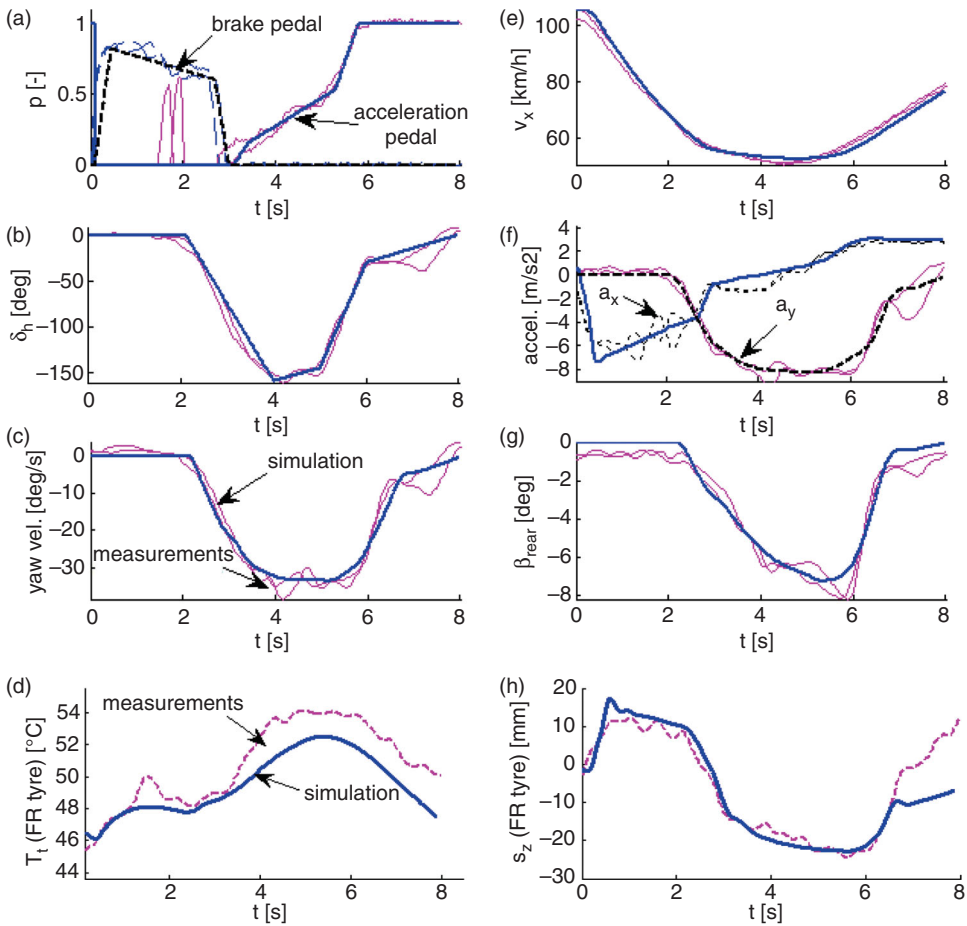


Figure 6. Comparison of time results from road tests and base line (c0) simulations of extreme RH corner negotiation.

linear piece-wise functions and incorporated as the model inputs (Figure 3). The additional three coefficients describing tyre thermodynamics (in Equation (2)), are estimated as: $H = 350 \text{ J/K}$, $k_1 = 5 \text{ W/K}$, $k_2 = 1 \text{ s/m}$.

High adequacy of the formulated ‘miMa’ model may be confirmed by evaluating the seven motion states (Figure 6), including temperature on the FR tyre tread, and the simultaneously obtained trajectory (Figure 5), which is in accordance with the track boundaries.

3. Optimisation task of driver actions for RH corner

3.1. Definition of multi-criteria optimisation

The described above closed-loop manoeuvre with RH corner (Figure 5) will be evaluated with respect to a sport performance by using two criteria: section lap time (t_{AB}) and exit velocity (v_B) at the section end. Which one is more important depends on a following part

of the racing track. In case when the corner leads to a longer straight, the exit velocity (v_B) is getting more important.

The optimisation algorithm of the driver actions in the considered manoeuvre is defined as follows:

- minimise the driver-vehicle performance criteria

$$\mathbf{w} = [t_{AB} - v_B]_{1 \times 1}, \quad (3)$$

- through decision variables

$$\mathbf{d} = [\delta_h \delta_b \delta_a]_{1 \times 16}, \quad (4)$$

- under constraints

$$\mathbf{d}_{\min} < \mathbf{d} < \mathbf{d}_{\max}, \quad (5)$$

- radial deviation less than ± 0.5 m of three trajectory reference points (braking, apex and exit);
- braking without full lock ($\dot{\varphi}_i > 0$, $i = 1:4$);
- braking with right foot (time delay between brake and accelerator application);
- vehicle spin is rejected ($|\dot{\psi}| < 60$ deg/s).

The actual driver actions, acquired from the track, are parameterised by linear piece-wise functions of time. For example, the brake pedal position (δ_b in Figure 6(a)) is parameterised in four knots by

$$\delta_b = [t_{b,1} \ t_{b,2} \ \delta_{b,2} \ t_{b,3} \ \delta_{b,3} \ t_{b,4}]_{1 \times 6}. \quad (6)$$

Vector (6) includes six components with four time constants (of four knots) and two brake positions (in knots number 2 and 3). Combining all the driver actions, there are 16 components included in the optimisation as decision variables (4). In that way the driver adaptation is emulated, not assuming any driver model.

In order to investigate the influence of tyre tread temperatures on optimal race driver controls, the following three cases are analysed:

- (c1) tyres with invariable grip vs. temp. characteristics (Figure 2, with $\mu_{\max} = 1$) (cyan colour),
- (c2) initially not warmed tyres with parabolic grip vs. temp. on cold day (Figure 2, $\mu_{\max} = 1.05$, $T_{i,0} = 0^\circ\text{C}$, $T_A = 0^\circ\text{C}$) (green colour),
- (c3) initially overheated tyres with parabolic grip vs. temp. on hot day (Figure 2, $\mu_{\max} = 1.05$, $T_{i,0} = 100^\circ\text{C}$, $T_A = 40^\circ\text{C}$) (red colour).

The temperatures of the BMW tyre tread, obtained from simulation of c2 and c3 cases, are presented in Figure 7 in time domain. In conditions (c2) of not warmed tyres on a cold day ($T_A = 0^\circ\text{C}$) temperatures increase from initial 0°C to maximal 80°C for the FL (outside) wheel and to 60°C for the RL wheel. The tyres heat up mainly during cornering phase in proportion to the side slip and the normal load. The peak temperature on FL loaded tyre is delayed by 1.5 s with respect to the corner apex ($t = 4$ s in Figure 7). Even a greater delay (2.5 s) is noticeable for the peak temperatures on the BMW rear axle, which

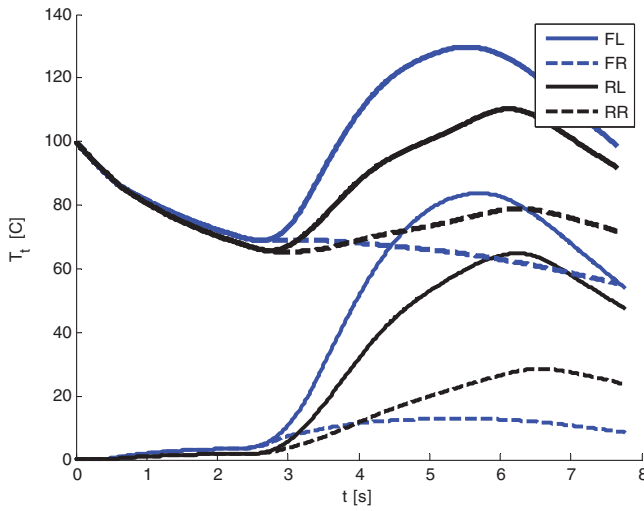


Figure 7. Temperatures of tyres tread during RH corner with the BMW ‘miMa’ model for c2 and c3 cases.

is drifted slightly at the corner exit. Analogous characteristics are obtained for initially warmed tyres (c3) on a hot day ($T_A = 40^\circ\text{C}$). Despite of braking in the first phase, the tyres cool down (from 100°C to 70°C) due to 60°C difference between the tyres and environment. In cornering phase, the temperature on the FL wheel increases by 60°C , reaching peak at 130°C .

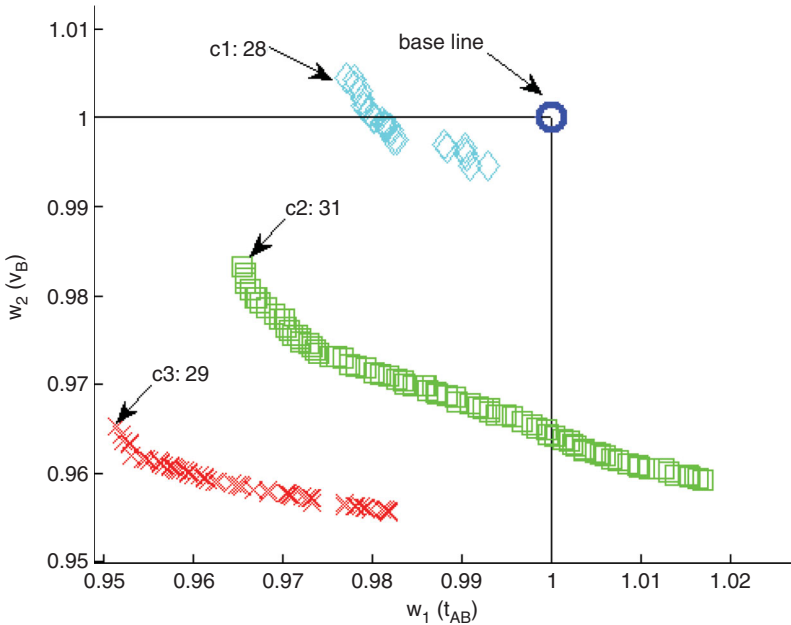


Figure 8. Pareto-optimal results of c1, c2 and c3 cases of RH corner with BMW E36.

This multi-criteria optimisation is solved by using genetic algorithms with non-dominated sorting,[11] which is effective in finding of global optima of discontinues objective spaces.

Owing to a high computational effectiveness of the formulated ‘miMa’ model described by 30 ODE (first- and second-order) of medium stiffness, the simulation time of the single manoeuvre of 8 s duration takes about 3 s on common PC (3 GHz, 2GB RAM). About 30,000 iterations (20 h) are needed to finish the optimisation with satisfying results.

Obtained Pareto-optimal fronts in c_1 , c_2 and c_3 cases, are presented in Figure 8 in normalised $w_1 - w_2$ plane. The base line (c_0) simulation is scored by ones in both criteria. Any improvement may be expected for the solution with lower criterion number.

The convex front of Pareto-optimal results (Figure 8) means contradictory relation between the criteria, i.e. the driver may decrease the time of passing this section or increase

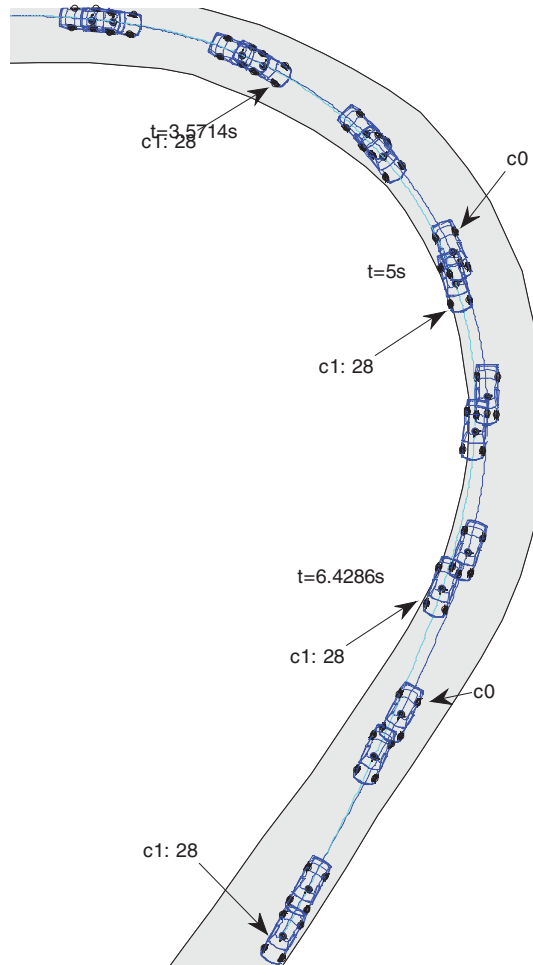


Figure 9. Pareto-optimal results of c_1 case (left) and comparison of base line (c_0) and optimal $c_1:28$ trajectories of BMW E36.

the exit velocity of the car. In dependence on the driver preferences and a type of following parts of the racing track, different solution can be chosen.

3.2. Optimised driver actions for tyres independent on temperature

For example, choosing the optimal solution c1:28 (Figure 8) the driver can maximally decrease the section time (t_{AB}) by 2.5% at expense of exit velocity (v_B) by 0.5% with respect to the base line (c0). Corresponding trajectories of the BMW E36 in c0 and c1:28 cases are presented in Figure 9.

The both racing lines are very similar. The optimised trajectory is slightly tighter crossing the corner apex closer. Further change in the motion trajectory (radial deviation greater than ± 0.5 m) is not permitted by the optimisation constraints (5). In c1:28 case, the vehicle achieves a lead by half-car length just after the braking phase. This lead is further increased, giving a full-car length advantage at the section end.

A comparison of time traces of the RH corner manoeuvre with the BMW E36 for the base line setup (c0) and the optimal solution (c1:28), is presented in Figure 10. The vehicle model with optimised driver actions achieves a slightly higher velocity (v_x) at each phase (entry, apex and exit) of the manoeuvre, what combined with the somewhat tighter trajectory (Figure 9) gives a reduction of the section time by 2.5%. This goal is obtained by: (i) delayed braking: (ii) greater steering wheel angle (δ_h) in the first phase and (iii) accelerator

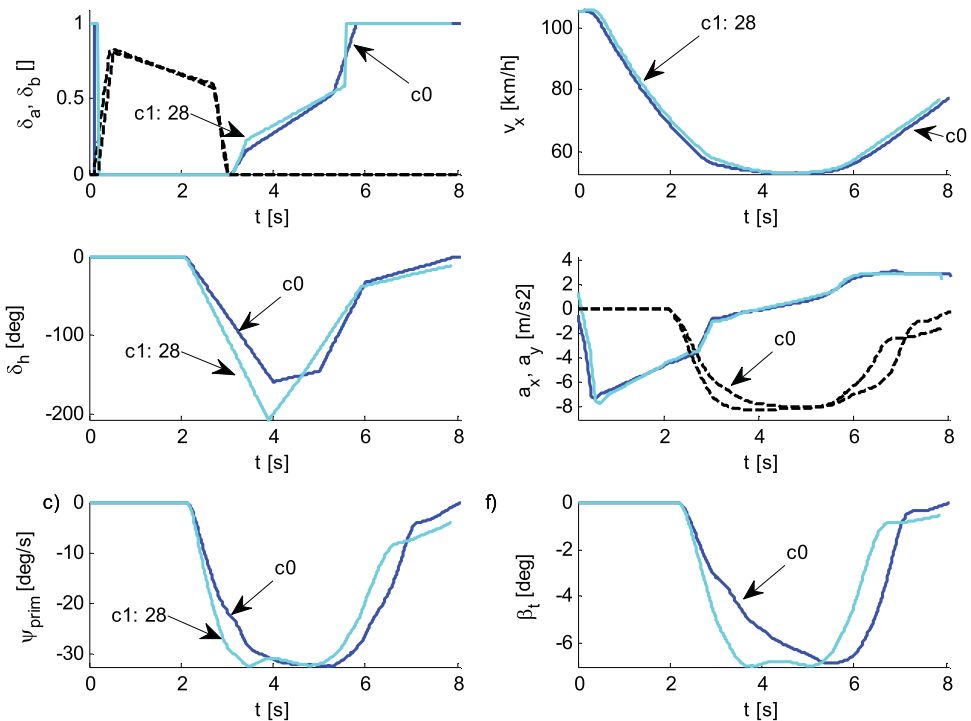


Figure 10. Comparison of time traces of RH corner manoeuvre with BMW E36 for base line (c0) and optimal (c1:28) driver actions.

control (δ_a). Thus, the lateral acceleration (a_y) and the rear axle side slip (β_{rear}) increased slightly at the corner entry, giving an opportunity to apply the throttle faster in the second part of the corner.

3.3. Optimised driver actions for initially not warmed tyres

The obtained Pareto-optimal front in c2 case is presented in Figure 8 together with the above discussed results of c1 case. Extreme solutions for not warmed tyres (c2) are better than the previous case, both in the lap time and in the exit velocity. For example, choosing the optimal solution c2:31 the driver can improve at the same time the section time by 1% and the exit velocity by 2%, comparing to c1:28 case. Corresponding trajectories of the BMW E36 in c1:28 and c2:31 cases are very similar, due to the optimisation constraints, therefore are not presented here.

A comparison of time traces of the RH corner manoeuvre with the BMW E36 for optimal solutions c1:28 and c2:31, is presented in Figure 11. The main consequence of initially cold tyres (Figure 7) is that during the first phase of the manoeuvre the tyre friction coefficient is 5% lower than in c1 case. Thus, the driver cannot brake so much (extreme deceleration decreased from 7.8 to 5.8 m/s² in Figure 11(e)) and steer (extreme steering angle decreased from 200 to 160° in Figure 11(b)). Taking into account a deterioration of the tyres grip, the first phase of the manoeuvre should be worse than c1. But, this is not the case. The driver with optimised actions (c2:31) takes advantage of changed balance

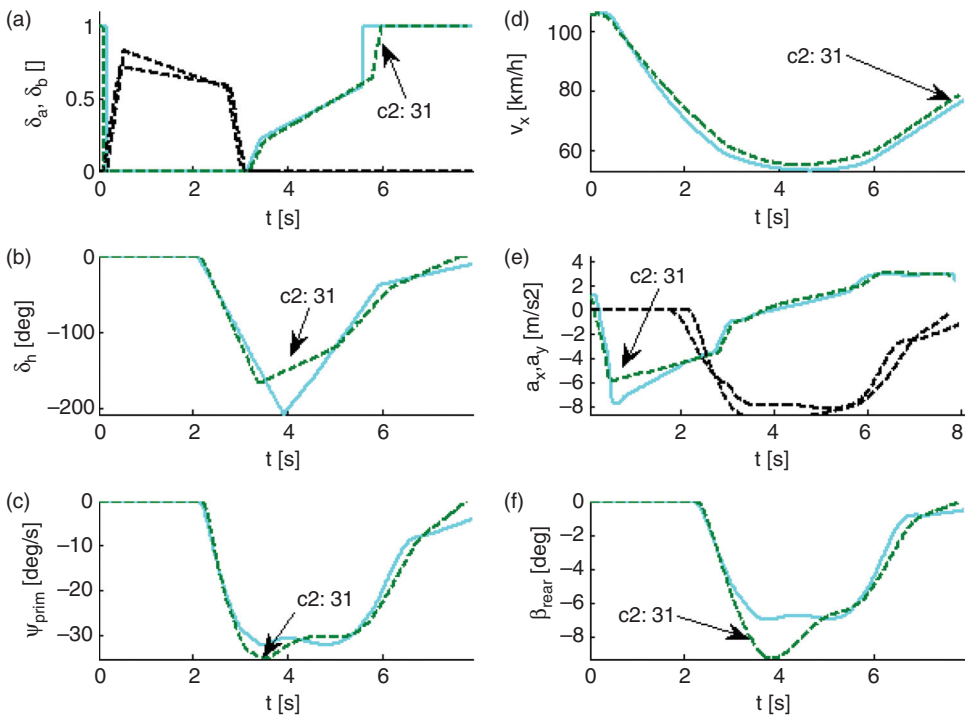


Figure 11. Comparison of time traces of RH corner manoeuvre with BMW E36 for optimal c1:28 and c2:31 driver actions.

of the vehicle, which is less understeering (more loose) on not warmed tyres. Therefore, the turn in process is improved by generation of a higher side slip angle (β_{rear}) on the rear axle.

As the tyre are heated during the second phase of the manoeuvre, they reach the optimum grip point (between $60 \div 80^\circ\text{C}$), where the tyre friction coefficient is 5% higher than in c1 case (Figure 7). This enables to finish the manoeuvre on the track and maintaining the gains in section time and exit velocity (Figure 11(d)).

3.4. Optimised driver actions for initially hot tyres

The obtained Pareto-optimal front in c3 case is presented in Figure 8 together with the above-discussed results of c1 and c2 cases. Extreme solutions for initially hot tyres (c3) and parabolic grip vs. temperature are even better than the previous cases with respect to lap time and exit velocity. For example, choosing the optimal solution c3:29, the driver can further improve both the section time by 1.5% and the exit velocity by 2%, comparing to the best previous c2:31 case.

A comparison of time traces of the RH corner manoeuvre with the BMW E36 for the optimal solutions c2:31 and c3:29, is presented in Figure 12. The mentioned above advantage, obtained in the optimisation of c3 case with initially overheated tyres, may

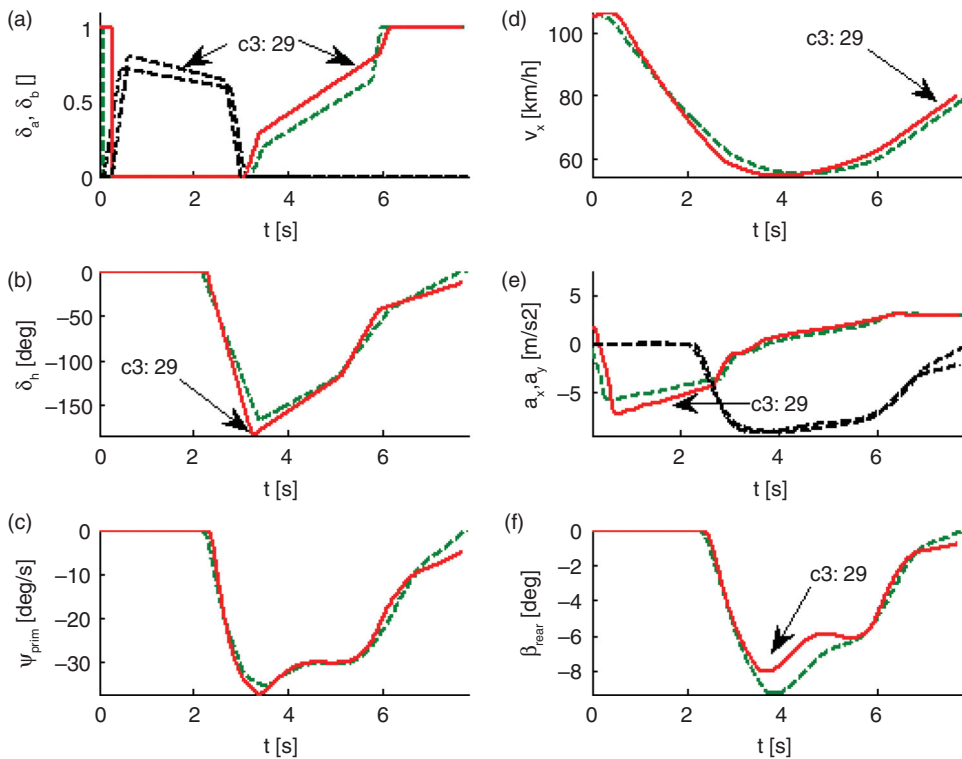


Figure 12. Comparison of time traces of RH corner manoeuvre with BMW E36 for optimal c2:31 and c3:29 driver actions.

be explained as follows. The temperatures of all the tyres are stabilised (Figure 7) by the driver actions in the optimal grip window between 60°C and 130°C (Figure 2) for the whole manoeuvre. The optimised driver (c3:29 in Figure 12) better controls the braking process and the drift angle during acceleration phase to avoid the tyres overheating. At the same time, the higher friction coefficient of the tyres is fully utilised, which brings noticeable improvements in the section time and the exit velocity (Figure 12(d)).

4. Conclusions

The paper presents the optimisation results of race driver actions during extreme negotiation of a RH corner with BMW E36 (Rear Wheel Drive, 200HP). Special emphasis is put on the driver adaptation to the influence of variable temperature of semi-slick tyre tread, which is described by the assumed characteristics of peak friction vs. temperature with the parabolic shape.

Other known approaches for tackling optimal lap time tasks, like optimal control methods, may be limited in real motorsport applications by:

- oversimplified driver models (artificial response of the driver);
- oversimplified vehicle models (deficient in parameters which are significant in motorsport);
- prohibitive computation time.

In the proposed approach here, the actual race driver actions (describing usage of steering wheel, brake and accelerator pedals) are acquired from the race track and parameterised by piece-wise functions of time. These parameters are then included as decision variables (with 16 components) for optimisation of the closed-loop manoeuvre. In that way the driver adaptation is emulated without a simplified driver model.

The ‘miMa’ vehicle model with 30 state variables and more than 400 parameters is formulated for optimisation purposes. In that way, it is possible to describe details of chassis components (relevant in motorsport) at a reasonable computational time (three times shorter than real time). Similar results are rarely achievable with commercial general purpose software.

The Magic Formula for quasi-static tyre tangential forces is extended in ‘miMa’ by the tyre thermodynamics model with the single lumped system. Heat is generated in the tyre contact patch due to a slip and can be exchanged with an environment by a convection. The utilised ‘miMa’ model is verified on the basis of track tests.

The optimisation goal function included two criteria: (w_1) section lap time and (w_2) vehicle velocity at the corner exit. The problem constraints included a fixed trajectory of motion in order to concentrate the paper scope on the driver actions only. This multi-criteria optimisation is solved by using genetic algorithms with non-dominated sorting. About 30,000 of iterations (20 h on regular PC) are needed to terminate with satisfying results. The obtained results are given on Pareto-optimal planes.

The following three cases of optimisation are investigated: (c1) tyres with invariable grip vs. temperature characteristics (with $\mu_{\max} = 1$), (c2) initially not warmed tyres ($T_{t,i} = 0^\circ\text{C}$, $i = 1, 2 \dots 4$) with the parabolic characteristics (with $\mu_{\max} = 1.05$ at $T_t = 80^\circ\text{C}$), and (c3) initially hot tyres ($T_{t,i} = 100^\circ\text{C}$, $i = 1, 2 \dots 4$) with the same

characteristics as in c2. In all of the cases, the obtained Pareto-optimal fronts confirm a trade-off character between the defined criteria. It means that the vehicle should be driven in a different way, depending on whether shorter lap time (w_1) or greater exit velocity (w_2) is more crucial. This should be related with a driving strategy for the next section of the racing track.

Although, the optimisation results strongly depends on the vehicle type, the ambient conditions and the assumed tyre grip characteristics, which are not known exactly, some general recommendation for performance drivers may be given as follows. In case of initially not warmed tyres, the driver should not brake or steer too much in the beginning, awaiting for an increased grip coming as the tyres heat up in the second phase of the manoeuvre. The driver can also take the advantage of changed balance of the vehicle, usually to more loose (less understeer), to initiate the turn-in and heat up the tyres more effectively. In other case of initially overheated tyres, the driver should better control the braking process and the drift angle during acceleration phase to sustain the tyres temperature in optimal grip window. The described strategy is typical for performance driving of a RWD vehicle.

The formulated algorithm of 'miMa' model optimisation proved to be useful for indicating a race driver how the driving strategy could be changed. The obtained time responses of steering wheel angle, brake and accelerator positions look very reasonable, owing to an innovative description of real driver actions, without any driver model controller. This approach seems to be suited for racing drivers especially, who are smooth and minimalistic on the controls.

The utilised tyre model, based on substitute mass thermodynamics, seems to be the simplest way to include a dynamic relation between tread temperature and tyre grip. The model is described by one first-order ordinary differential equation and four parameters, what is beneficial in optimisation applications. Further development of the considered tyre model can lead to an increase in computational complexity (estimation and execution time), still maintaining semi-physical sense hard for interpretation. The following improvements may include:

- tyre cornering stiffness as function of the tyre temperature (important in a linear range of vehicle handling);
- heat generation due to the tyre internal work derived from the tyre deflections;
- multi rib tread model (with 3–5 ribs), which enables to differentiate between temperatures of inner, mid and outside part of the tyre tread as effect of e.g. the camber angle;
- additional substitute mass of the tyre structure (carcass, bend and internal air) that can relate heating process with internal air pressure.

In the cases of not warmed or overheated tyres a performance driver should change not only his driving technique, but the vehicle motion trajectory should also be adapted. In order to limit the paper scope, this situation was excluded from the optimisation by proper definition of the constraints function. The formulated computational environment with the 'miMA' vehicle model enables a mutual optimisation of the driver actions, the vehicle motion trajectory and the vehicle chassis parameters. These are key features for actual motorsport applications.

The developed algorithm, as a result of high computational effectiveness of the ‘miMa’ vehicle model, can be implemented for a more complex manoeuvres at a racing track. Optimisation of a full lap problem is still a challenge.

Disclosure statement

No potential conflict of interest was reported by the author.

References

- [1] Van Valkenburgh P. Race car engineering and mechanics. Los Angeles: HP Books; 2002.
- [2] Milliken W, Milliken D. Race car vehicle dynamics. Warrendale, PA: Society of Automotive Engineers (SAE) International; 1995.
- [3] Février P. Thermal and mechanical tire force & moment model presentation. Paper presented at the 4th Intelligent Tire Technology Automotive Conference, Wiesbaden; 2008.
- [4] Haney P. The racing & high – performance tire: using the tire to tune for grip & balance. Springfield: TV Motorsports; 2003.
- [5] Mizuno M. Development of tire side force model based on “Magic Formula” with the influence of tire surface temperature. R&D Review of Toyota CRDL. 2003;38(4):17–22.
- [6] Chaligné S. Tire thermal analysis and modelling [Master’s thesis]. Göteborg: Chalmers University of Technology; 2011.
- [7] Trevorror N, Gearing R. MuRiTire – real time simulation of distributed contact patch forces, moments and temperatures. Guildford: 4th International Tyre Colloquium; 2015.
- [8] Gipser M. FTire and puzzling tire physics: teacher, not student. Guildford: 4th International Tyre Colloquium; 2015.
- [9] Farroni F, Giordano D, Russo M, Timpone F. TRT: thermo racing tyre a physical model to predict the tyre temperature distribution. *Meccanica*. 2014;49:707–723.
- [10] Casanova D, Sharp RS, Symonds P. Minimum time manoeuvring: the significance of yaw inertia. *Veh Syst Dyn*. 2000;34:77–115.
- [11] Gobbi M, Mastinu G, Doniselli C. Optimising a car chassis. *Veh Syst Dyn*. 1999;32(2):149–170.
- [12] Kluziewicz M, Maniowski M. Comparison of race and rally driving techniques in cornering of FWD car. *Tech Trans*. 2012;5-M(10):51–62. Cracow Tech Univ.
- [13] Maniowski M. Optimization of wheel suspensions and driving control of FWD car for faster cornering. *Tech Trans*. 2012;5-M(10):35–50. Cracow Tech Univ.
- [14] Maniowski M. Research on controlled sliding utilized in drifting competitions. *Automotive Safety 2014: IX International Science-Technical Conference, Rajecské Teplice-Slovakia*; 2014.
- [15] Maniowski M. Optimization of spring–damper modules of rally car for fast passing over jump inducing bumps. Manchester: International Association of Vehicle System Dynamics; 2011.
- [16] Knapczyk J, Maniowski M. Elastokinematic modeling and study of five-rod suspension with subframe. *Mech Machine Theory*. 2006;41:1031–1047.
- [17] Knapczyk J, Maniowski M. Synthesis of a five-rod suspension for given load-displacement characteristics. *Proc Instn Mech Engrs, Part D: J Automobile Eng*. 2006;220:879–889.
- [18] Pacejka H. Tire and vehicle dynamics. Oxford: Butterworth-Heinemann; 2012.